Published in Journal of Modern Optics 45, issue 7, 1395-1403, 1998
which should be used for any reference to this work

Rigorous diffraction theory applied to microlenses

P. BLATTNER† and H. P. HERZIG
Institute of Microtechnology, University of Neuchâtel, Rue Breguet 2, 2000 Neuchâtel, Switzerland

Abstract. In this paper, we discuss the behaviour of small cylindrical microlenses, arranged in one-dimensional arrays and as single elements. For this purpose, we apply a standard rigorous diffraction theory, commonly used for diffraction gratings. We investigate the coupling effect between the elements. It turns out that single elements behave like periodic elements if the spacing is chosen correctly. Furthermore, we compute the complex transmission function by rigorous diffraction theory and compare them with classical theories (combined ray tracing and the thin-element approach). Finally, we discuss the focal properties of microlenses in the rigorous regime.

1. Introduction

Today's technology allows the realization of small microlenses which have geometrical dimensions of the order of a few wavelengths (figure 1). These lenses are typically realized by the reflow technique [1] and have perfect spherical surfaces. In standard lens design, mainly two approaches are applied to describe the behaviour of such elements. One method is ray tracing and the other is the thin-element approach. In its simplest version, ray tracing applies the laws of refraction and reflection to individual rays. No diffraction effects are taken into account. However, it is possible to include the optical path length through the optical elements (phase-sensitive ray tracing). This allows one to determine the field in the plane of the exit pupil of an optical system. In a second step, the free-space propagation of the field can be computed by diffraction theory (angular spectrum, Rayleigh–Sommerfeld or Fresnel). This method is referred to as *combined* ray tracing [2]. In the thin-element approach, the plane of the entrance pupil and the plane of the exit pupil coincide. In this case, the element alters only the phase of the incident wave, that is the wave is delayed proportionally to the surface relief of the element.

The classical theories lose their validity if the geometrical dimensions of the element are of the order of the wavelength. For this purpose, different rigorous diffraction theories have been investigated in the past. They are based on either the integral or the differential representation of the wave equation. In the literature, only a few examples are presented for the rigorous computation of microlenses. Most of them are valid for diffractive microlenses [3, 4]. Rigorous computation of refractive microlenses based on intergral boundary methods and applied to have been presented by Tabbara [5] and more recently by Wang and Prata [6].

† email: peter.blattner@imt.unine.ch

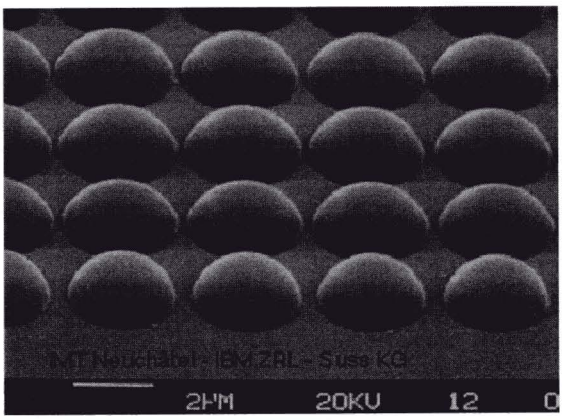

Figure 1. Scanning electron microscopy picture of an array of very small microlenses (diameter, about 3 µm) [1].

However, these calculations are cumbersome and have been restricted to single elements. On the other hand, there exist efficient rigorous theories valid for periodic structures only [7–9]. They are mainly used to predict the diffraction efficiency of high-frequency gratings.

In this paper, we apply the rigorous eigenmode method to microlens arrays [10]. We restrict the analysis to arrays of continuous relief lenses illuminated with a plane wave (two dimensions and transverse electric polarization). Furthermore, we analyse the diffraction at single elements by introducing a large spacing between the elements and we discuss the coupling effects between the elements. We compare the transfer function of microlenses calculated by rigorous diffraction theory and two classical theories (combined ray tracing and the thin-element approach). Finally, we investigate the focusing properties of microlenses.

2. Rigorous diffraction theory

Illuminating periodically arranged elements by a plane wave results in a discrete plane-wave spectrum. Therefore, the field can be written as

$$U_T(x, z) = \sum_{m=-\infty}^{\infty} T_m \exp\left[i(k_{xm}x + k_{zm}z)\right], \tag{1}$$

where k_{xm} and k_{zm} are the projections of the associate plane wave wave-vector $\mathbf{k}_m$ onto the x and z axis respectively. The diffraction problem consists in finding the amplitudes T_m of the individual plane waves (or diffraction orders). In the rigorous eigenmode method [10] the periodically modulated surface structure or, in our case, the periodically arranged scatters are divided into a stack of thin films. The total number of layers depends on the thickness-to-wavelength ratio. We typically chose $25 \times h/\lambda$ layers, where h is the thickness of the structure and λ the wavelength. The dielectric constant distribution $\epsilon(x, z) = \epsilon_n(x, z_n)$ of each film is expanded into a Fourier series, and the electric field into eigenmode functions. Introducing these expansions in the wave equation results in an eigenvalue system that can be easily solved. The dimension of the eigenvalue system depends on the

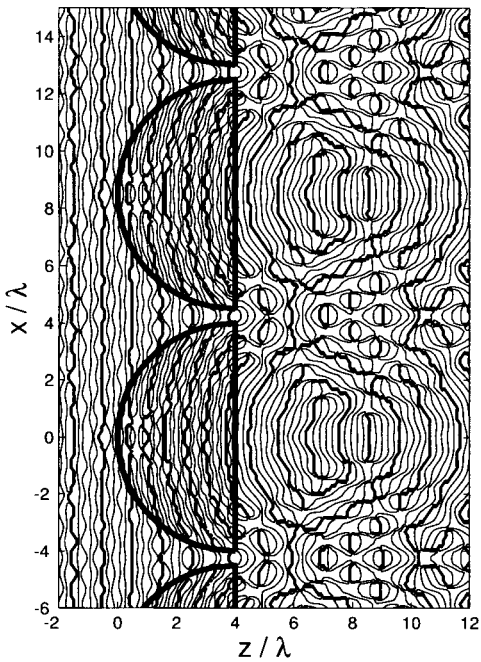

Figure 2. Calculated near-field phase contour plot of a microlens array. The elements have a diameter of 8λ, a height of 4λ and a refrative index $n = 1.5$. The array is illuminated by a TE-polarized plane wave, with perpendicular incidence.

grating period-to-wavelength ratio. It has been shown that for dielectric structures all propagating diffraction orders and some few evanescent diffraction orders (typically ten) have to be retained in the analysis [10]. Once the eigenvalues are determined, the amplitudes of the eigenmode functions are found by matching the electromagnetic boundary conditions.

With this method, it is possible to find the rigorous complex transmission function of any periodic structure, and in particular also the light distribution in the near field of microlens arrays (figure 2).

In the following, we show how the method can be applied to modelling a single microlens. There are mainly two points to consider when comparing microlens arrays with single elements. First, there are interference effects during the free-space propagation between the elements (e.g. the self-imaging effect or the Talbot effect).

Secondly, since the geometrical dimensions are small, the individual lenses couple with each other (intrinsic coupling). The coupling influence can be illustrated by comparing the rigorous transmission function of periodically arranged elements with the rigorous transmission function of a single element. Unfortunately, there exist only a few analytic (rigorous) solutions for the interaction of light with single elements. One case is the diffraction at a cylinder (figure 3). In that case, it is possible to express the field outside the cylinder by a superposition of Bessel and Hankel functions (for example [11])

$$U_{\text{single}}(r,\theta) = U_0 \sum_{n=-\infty}^{\infty} (-\mathrm{i})^n \exp(\mathrm{i}n\theta)[J_n(kr)A_n + H_n^{(2)}(kr)B_n]. \tag{2}$$

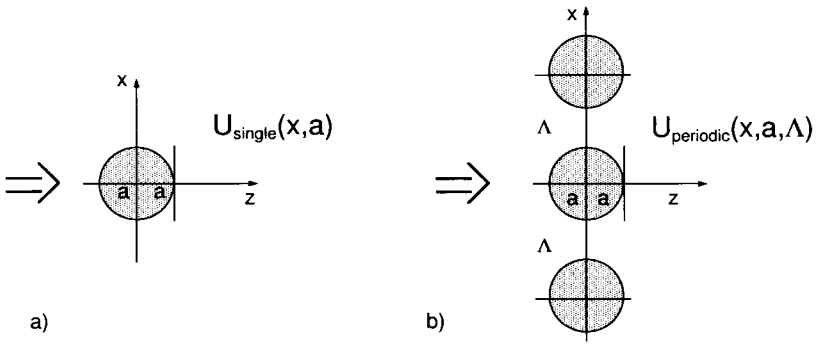

Figure 3. Configuration used to illustrate the coupling effect between elements. (*a*) The calculated field U_{single} of a cylinder illuminated with a plane wave is compared with (*b*) the field of periodically arranged cylinders U_{periodic}.

A_n and B_n are coefficients which depend on the diameter of the cylinder and the indices of refraction of the cylinder and the surrounding area. In parallel to that, we compute the field generated by periodically arranged cylinders with the method presented before. We denote this field by $U_{\text{periodic}}(x, y) = U_{\text{T}}$. The coupling parameter χ is now defined as the difference between the fields U_{single} and U_{periodic} in the output plane, integrated over a fixed interval of one wavelength:

$$\chi(\Lambda) = \int_{x=-\lambda/2}^{\lambda/2} |U_{\text{single}}(x, a) - U_{\text{periodic}}(x, a, \Lambda)|^2 \, \mathrm{d}x, \tag{3}$$

where Λ is the grating period of the microlens array. Figure 4 illustrates the coupling coefficient χ in function of the grating period Λ for different diameters of the cylinders. It it interesting to observe that a resonance occurs if the grating period is a multiple of the wavelength. Furthermore, the coupling effect is larger for small cylinders than for large cylinders. For very small structures the coupling may occur even if the elements are spaced by several wavelengths. To understand this behaviour, we compute the spectrum of (single) cylinders of different diameters. If the size of the cylinders are large (figure 5), the spectrum is mainly given by the propagating frequencies, that is $|k_x| < k = 2\pi/\lambda$. For small cylinders (figure 6), the spectrum is mainly given by the spatial frequencies around $\pm k$, that is they correspond to evanescent waves (or surface waves) of wavelength λ, also called critical evanescent waves. If the elements are arranged periodically, the spectrum becomes discrete. Depending on the grating period it is possible that the sampling falls directly on the critical frequencies $k_x = \pm k$. In this case, there is maximum coupling between the elements. In addition the diffraction pattern becomes dominated by the two surface waves (in the positive and negative directions). This is due to the large penetration depth† of the evanescent waves.

It turned out that it is possible to simulate the diffraction of a single element with the help of a grating diffraction theory, if the grating period is chosen correctly. First, the grating period should not be a multiple of the wavelength

† The penetration depth of an evanescent wave is defined as $z_{\text{eff}} = 1/\gamma$, with $\gamma = (k_x^2 - k^2)^{1/2}$. For a critical evanescent wave ($k_x = k$), z_{eff} becomes infinite!

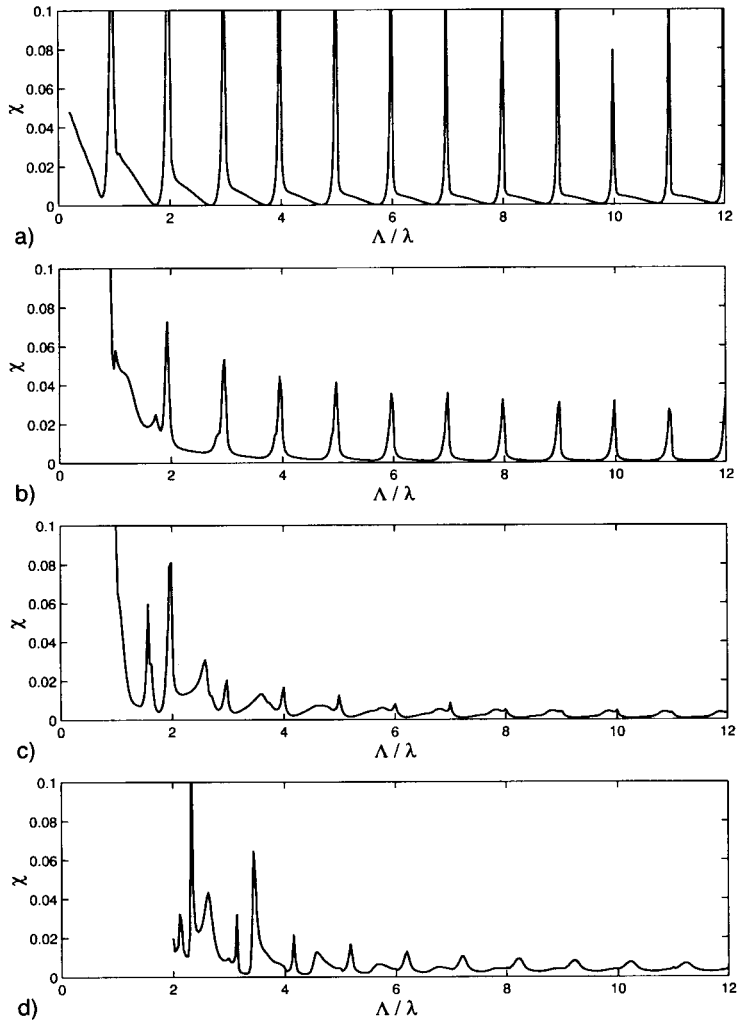

Figure 4. Coupling coefficient χ (equation (3)) against grating period Λ for different diameters 2a of the cylinders: (*a*) $2a = \lambda/5$; (*b*) $2a = \lambda/2$; (*c*) $2a = \lambda$; (*d*) $2a = 2\lambda$. The coupling coefficient shows a resonance if the grating period is a multiple of the wavelength. The smaller cylinders in (*a*) show larger coupling effects than the larger cylinders in (*b*) do.

and, second, the period should be larger than twice the diameter of the element. This result is justified by figure 4.

3. Comparison of classical and rigorous theories

In this section we compare classical and rigorous diffraction theory applied to two different microlenses: a thick ($h = 2\lambda$) and thin ($h = \lambda/5$) cylinder lens of the same diameter $2a = 4\lambda$. In this context, the terms *thick* and *thin* are referred to paraxial and non-paraxial elements, that is to small and large deflection angles respectively. In our case the deflection angles at the border of the element are 41.8°

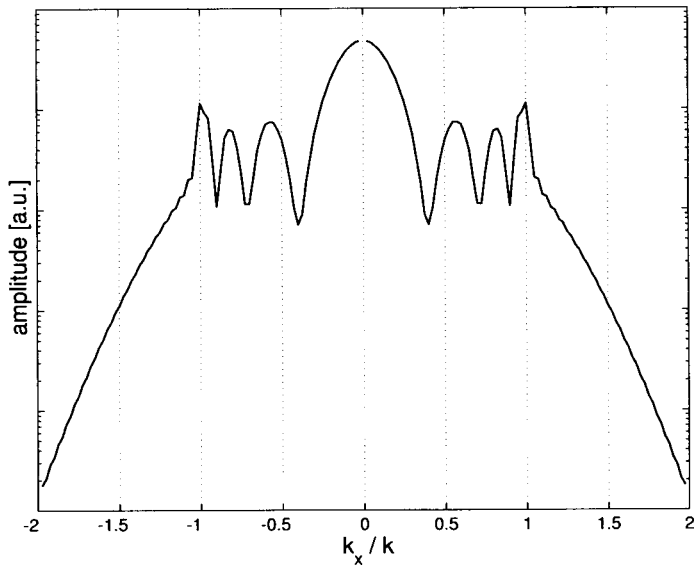

Figure 5. Spectrum of a cylinder of diameter $2a = 3\lambda$ (a.u., arbitrary units). Frequencies $|k_x|$ larger than $k = 2\pi/\lambda$ correspond to evanescent waves. The spectrum of such a large cylinder is mainly given by the propagating waves ($|k_x| < k$).

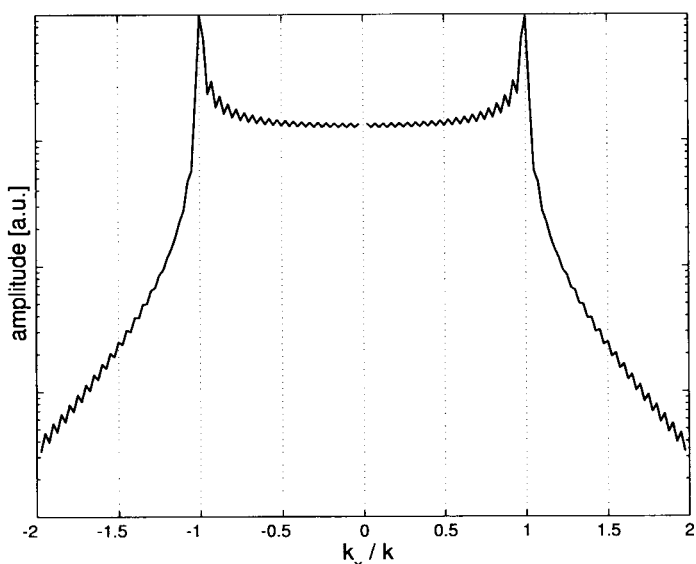

Figure 6. Spectrum of a cylinder of diameter $2a = \lambda/2$ (a.u., arbitrary units). The spectrum of such a small cylinder is mainly given by the critical evanescent waves of frequency $k_x = \pm k$.

(thick) and 7.5° (thin). It turns out that the spectrum of thin lenses (figure 7) calculated by the classical theories (combined ray tracing and the thin-element approach) agree well with the rigorous computations. In this case, the influence of the thin element on the wave front is small and the diffraction pattern is mainly

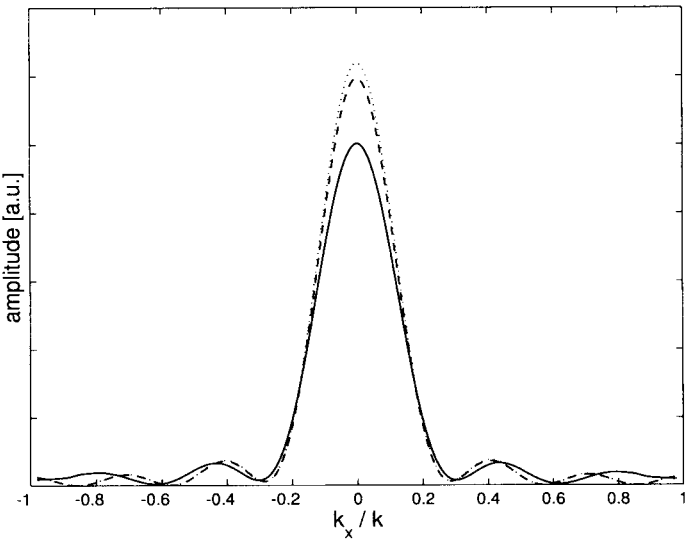

Figure 7. Calculated spectrum of a thin lens (a.u., arbitrary units): (——), rigorous computation; (– – –), ray tracing; (· · · · ·), the thin-element approach. The lens has a diameter of $2a = 4\lambda$ and a thickness of $h = \lambda/5$.

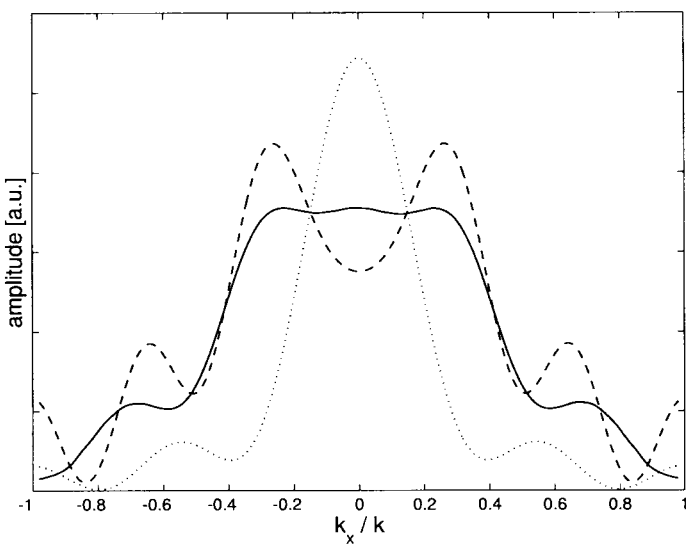

Figure 8. Calculated spectrum of a thick lens (a.u., arbitrary units): (——), the rigorous computaiton; (– – –), ray tracing; (· · · · ·), the thin-element appraoch. The lens has a diameter of $2a = 4\lambda$ and a thickness of $h = 2\lambda$.

given by the aperture, that is the spectrum has a *sinc* form. The only difference between the theories is in the absolute intensities. The thin-element approach and ray tracing show higher intensities, because there are no losses in the transmission functions (only the phase is affected).

In the case of the thick element (figure 8), the prediction made by the thin-element approach is wrong. The theory does not predict the bending of the border rays through the element. Therefore, the spectrum of the transmission function is

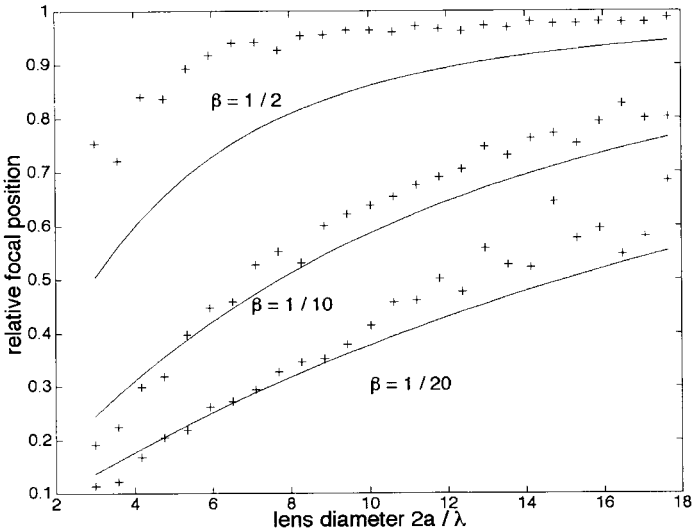

Figure 9. Illustration of the focal shift, where the focal position relative to the paraxial focal position in function of the diameter of the lens is plotted for different aspect ratios $\beta = h/2a$: (——), focal positions calculated by the thin-element approach; (+), the rigorous calculated focus positions.

too small! On the other hand, combined ray tracing shows smaller differences from the rigorous computations. One can conclude that combined ray tracing is more accurate than the thin-element approach and that the method is valid for elements with diameters down to few wavelengths.

4. Focal properties of microlenses

The thin element approach predicts a focal shift for elements having low Fresnel numbers [12]. The Fresnel number is defined as $N = a^2/\lambda f$, where f is the (paraxial) focal length of the lens. Microlenses, which have a diameter $2a$ of a few wavelengths are especially affected by this effect, because the minimum achievable focal length is $f_{\min} = a/(n-1) \approx 2a$, n being the refractive index of the lens. Thus, the maximum achievable Fresnel number is of the order of

$$N_{\max} \approx \frac{a}{2\lambda}. \tag{4}$$

This means that, owing to the small size, their properties are dominated by diffraction at the aperture. It has been shown in section 3 that the thin-element approach does not describe thick lenses sufficiently well. Hence, we expect a different behaviour of the rigorous computed focal shift than prediced by thin theory. Figure 9 illustrates the focal shift in function of the diameter of the lens for different aspect ratios β. The aspect ratio β is defined as the ratio of the lens thickness to the lens diameter, that is $\beta = h/2a$. For small aspect ratios the computations based on the thin-element approach agree well with the rigorous computations. For high aspect ratios (and as consequence also *thick* elements) there is quite a large difference between the two models. It turns out that the focal shift of thick lenses is less severe than predicted by the thin-element approach.

5. Conclusions

We have shown that it is possible to simulate single-element diffraction with the aid of a rigorous grating diffraction method by carefully choosing the grating period. Furthermore, we presented a comparison between three different methods to calculate the interaction of light with small lenses. For thin elements, all three methods predict well their behaviour, even for very small lenses. This is mainly because thin lenses are dominated by the edge diffraction which influences the focusing behaviour of the lens. We have shown that there is a good agreement between the classically predicted focal shift and rigorous computations.

For thick lenses, combined ray tracing is more precise than the thin-element approach. For such elements, the focal shift turned out to be less pronounced than predicted by the thin-element approach. In any case, it hs been illustrated that very small lenses also exhibit some focusing behaviour. This result is in a good agreement with the results presented by Wang and Prata [6].

Acknowledgment

This work has been supported by the Swiss priority program Optique II.

References

[1] Völkel, R., Herzig, H. P., Nussbaum, Ph., Blattner, P., Dändliker, R., Cullmann, E., and Hugle, W. B., 1997, *Microelectron. Engng*, **35,** 513.
[2] Stamnes, J. J., 1986, *Waves in Focal Regions* (Bristol: Adam Hilger).
[3] Hirayama, K., Glytsis, E. N., Gaylord, T. K., and Wilson, D. W., 1996, *J. opt. Soc. Am.* A, **13,** 2219.
[4] Schmitz, M., and Bryngdahl, O., 1997, *J. opt. Soc. Am.* A, **14,** 901.
[5] Tabbara, W., 1973, *J. opt. Soc. Am.*, **63,** 17.
[6] Wang, A., and Prata, A., Jr, 1995, *J. opt. Soc. Am.* A, **12,** 1161.
[7] Moharam, M. G., and Gaylord, T. K., 1982, *J. opt. Soc. Am.*, **72,** 1385.
[8] Li, L., 1993, *J. mod. Optics*, **40,** 553.
[9] Morf, R. H., 1995, *J. opt. Soc. Am.* A, **12,** 103.
[10] Turunen, J., 1997, *Micro-optics*, edited by H. P. Herzig (London: Taylor & Francis).
[11] Kozaki, S., 1982, *J. appl. Phys.*, **53,** 7195.
[12] Li, Y., and Wolf, E., 1981, *Optics Commun.*, **39,** 211.